ARCHIVES
of
FOUNDRY ENGINEERING

ISSN (2299-2944)
Volume 2024
Issue 1/2024

135 – 140

17/1

10.24425/afe.2024.149261

Published quarterly as the organ of the Foundry Commission of the Polish Academy of Sciences

Quality Control of Liquid Aluminium Alloy Using Thermal Imaging Camera

R. Władysiak
Lodz University of Technology, Department of Materials Engineering and Production Systems, Łódź, Poland
Corresponding author: E-mail address: ryszard.wladysiak@p.lodz.pl

Received 16.11.2023; accepted in revised form 06.02.2024; available online 21.03.2024

Abstract

This paper presents the results of a study on the use of infrared thermography to assess the quality of liquid metal, a basic semi-finished product used in foundry production. EN AC-46000 alloy with the designation AlSi9Cu3(Fe) was used for the study. The crystallization process of the alloy was investigated using the TDA method with a Crystaldigraph device and Optris PI thermal imaging camera. The research describes how to use a thermal imaging camera to assess the quality of aluminium alloys. These alloys, due to their propensity in the liquid state to oxidise and absorb hydrogen, a refining procedure in the melting process. The effects of alloy refining are evaluated during technological tests of hydrogen solubility, density and casting shrinkage. The results presented in this paper showed that there is a statistical correlation between the density of the metal and the temperature values from the thermogram of the sample, obtained during its solidification. The existing correlation makes it possible to develop a thermographic inspection algorithm that allows a fast and non-contact assessment of aluminium alloy quality.

Keywords: Thermal imaging camera, Aluminium alloy, Quality control

1. Introduction

The liquid metal preparation technology is an important step in the casting process. The process used mainly determines the properties of the casting obtained. Molten aluminium alloys, due to their high tendency to absorb gases in the liquid state, are exposed to contamination with hydrogen and metal oxides and porosity that reduces the density and functional properties of the casting [1, 2]. Obtaining castings with high properties requires the fulfilment of many conditions, starting with the selection of a suitable melting furnace, the use of covering materials to protect the melted metal from impurities and the use of appropriate modification and refining procedures for the liquid alloy. In the many refining methods used, a stream of refining gas bubbles (argon, nitrogen) is created in the liquid alloy, which, flowing through the refined metal, purify it from hydrogen, but also from oxides that constitute harmful solid impurities [3]. An essential element completing the alloy preparation process is the quality assessment. The refining efficiency of the produced alloy is assessed by gas dissolution degree of the alloy. This assessment can be made by observing the solidification process of the sample and the shape of the surface during solidification, or by the density of the sample and determination of the gas number [4]. The current method and equipment for density and gas number determination make these tests time-consuming, requiring specific samples of the alloy to be cast. They also require additional measurements of the weight of the sample immersed in water and then the density calculation of the alloy [5]. Another method that has been successfully used to assess the quality of liquid silumin and cast iron and to predict the mechanical properties of these alloys in castings is thermal and derivation analysis (TDA) [6-9]. In this method, the analysis of the solidification process was carried out using the Crystaldigraph. In contrast, the paper [10] presents the results of research confirming the possibility of conducting the thermal and derivative analysis of solidifying Al-

Si alloy using a thermal imaging camera. Compared to the traditional ATD method, the use of a high-frequency camera allows the recording of rapidly changing thermal processes typical of real die castings (Fig. 1).

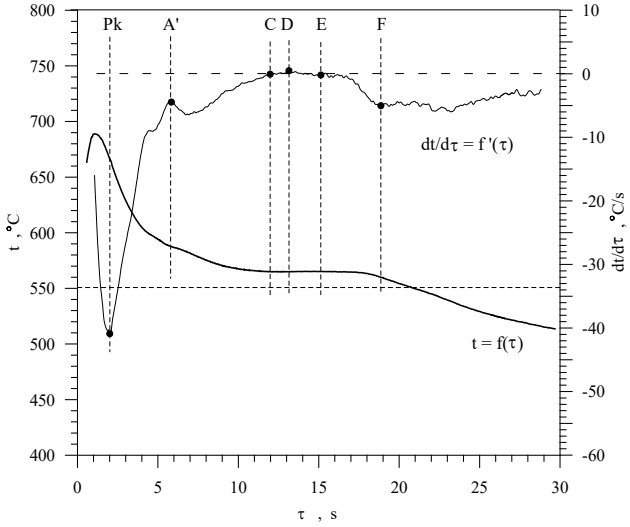

Fig. 1. Developed results from the Al-Si alloy crystallisation process using the Optris PI thermal imaging camera

The rapid development of thermography is resulting in increasingly high quality and availability of thermal imaging cameras. As a result, they are finding applications in many industries [11-15]. In addition to their basic advantage, which is the non-contact nature of the measurements made, they are also appreciated for the variety and wide temperature range of the objects tested, as well as the accuracy and speed of measurement. In view of the above, the aim of the described work was to investigate the possibility of assessing the density of a liquid Al-Si alloy on the basis of an thermographic analysis of sample surface during solidification of the alloy.

2. Materials and methods

The essence of the work was to carry out thermographic tests on alloy samples with varying degrees of gaseous and solid impurities, identified by alloy density. EN AC-46000 alloy with the designation AlSi9Cu3(Fe) was used for the study. The chemical composition of the alloy is shown in Table 1. The crystallization process of the alloy was investigated using the TDA method with a Crystaldigraph device from Z-Tech, Poland. It is a hypoeutectic Al-Si casting alloy with increased copper content, which is used for the manufacture of machine parts by die casting technology. The liquid alloy was prepared in an electric crucible furnace PT 900 (Czylok, Poland) with a crucible made of SiC. Alloy preparation consisted of melting and long-term annealing at 850 C. An increase of hydrogen solubility of alloy was achieved by periodically dispensing water mist under the free surface of the liquid metal during its overheating in the furnace. During the treatment of the alloy, its temperature decreased. The test specimens, whose shape and dimensions are shown in Figure 2, were poured at the temperature 680-700 C in an open casting die made of steel. During the cooling and solidification of the metal samples, observations of the metal surface in visible light and thermographic analysis were carried out using an OPTRIS PI thermal imaging camera from Optris GmbH and the dedicated Optris PI Connect software (Figure 3). In the study of infrared radiation, the radiometric values of the emissivity coefficient were analysed in the range 0.1÷0.4. The temperature was verified using a K thermocouple. The density of the samples was verified using the FMA Balance device, shown in Figure 4. The structure of the samples was analysed by macroscopic observation and microstructure evaluation using a Nikon Eclipse MA200 microscope.

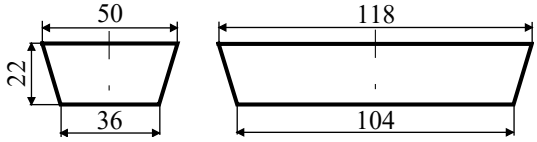

Fig. 2. Size and shape of the sample for thermographic testing

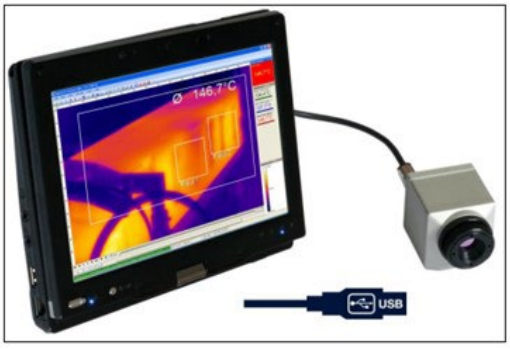

Fig. 3. Optris PI thermal imaging camera

Fig. 4. FMA Balance device

Table 1.
Chemical composition of EN AC-46000

Elements, weight %									
Si	Fe	Cu	Mn	Mg	Cr	Ni	Zn	Ti	Al
9.71	0.925	2.230	0.225	0.326	0.031	0.115	1.170	0.049	rest

3. Results of research

Figures 5 and 6 show the analysis of the alloy solidification process and the microstructure of the resulting sample. These studies show that the solidification of the alloy consists of three stages: cooling of the liquid metal, solidification and cooling of the liquid-solid mixture, and cooling of the solid phase. The crystallisation of a silumin sample starts with the pre-eutectic α (Al) phase - stage II. In stage III, the eutectic two phases (α+β) crystallises. The solidification of the alloy is completed by the crystallisation of multiple eutectics with Mg_2Si and Al_2Cu phases in stage IV. ATD analysis indicates that it is a near-eutectic alloy with a small solidification temperature range, favouring directional solidification in the casting.

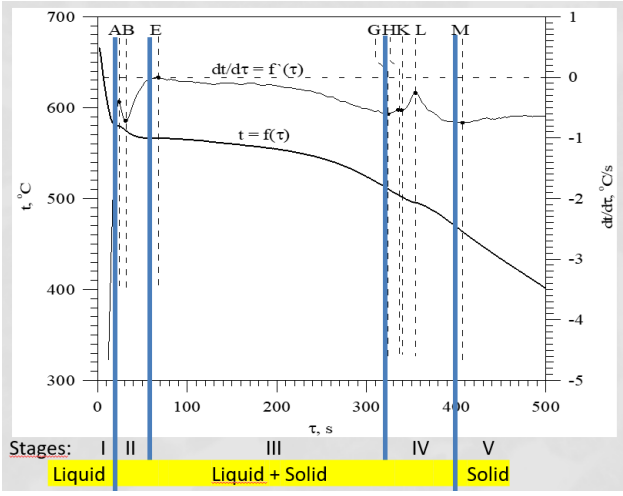

Fig. 5. Solidification process of the alloy by TDA method

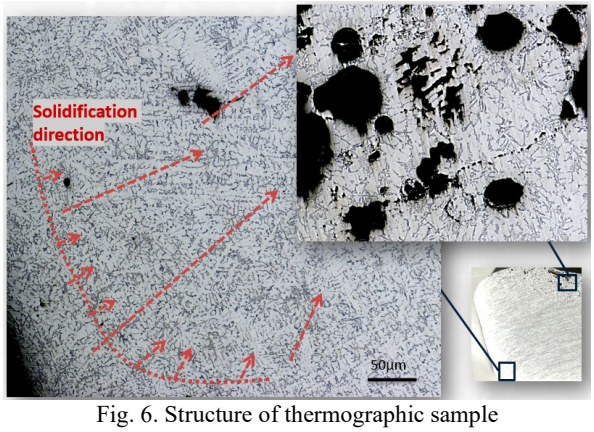

Fig. 6. Structure of thermographic sample

Analysis of the structure of the sample indicates that solidification occurs in a directional manner, which starts at the surface of the die walls with a thin layer of frozen crystals. Subsequently, the front of the crystallising columnar crystals moves towards the centre of the upper layer of the sample, while pushing down the impurities of the sample. The upper layer is dominated by equiaxial crystals with a high proportion of rows and gaseous porosity. This analysis indicates that such solidified samples may be suitable material for thermographic studies based on analysis of the top surface of the sample. Quantitative differences in porosity and impurities accumulated in the upper layer may be a factor determining the heat flux recorded by the thermal imaging camera.

Figure 7 shows a comparison of 3 representative samples with different alloy densities. The macroscopic analysis of the samples shows that there is a relationship between the shape of the upper sample surface, the cross-sectional structure and the alloy density. An increase in the area of impurities in the upper layer of the sample is accompanied by a decrease in alloy density.

Fig. 7. View and section of representative samples with alloy density ρ = 2.55 ÷ 2.69 g*cm^{-3}

Figure 8 shows the distribution of impurities in the sample structure as a function of alloy density and height of position in the sample. The study shows that a reduction in alloy density from 2.69 g*cm^{-3} to 2.55 g*cm^{-3} increases the area of micro shrinkage and porosity in the upper layer of the sample and, to a much lesser extent, increases the number of pores in the middle and lower layers of the test sample.

Figure 9 shows the change in shape, texture of the top surface of the sample during solidification. On the basis of the study, 4 main stages of sample surface changes were distinguished: mirror-like - in the liquid state (stage I), flat partly matt (stage II), partly matt and concave (stage III) and matt and concave - completely solidified (stage IV).

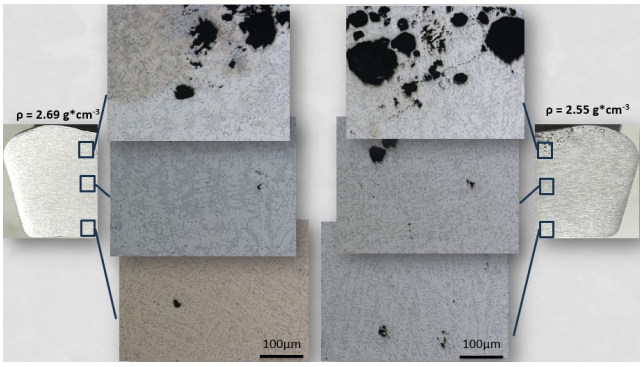

Fig. 8. Comparison of impurity distribution in alloy samples with density 2.69 g*cm^{-3} and 2.55 g*cm^{-3}

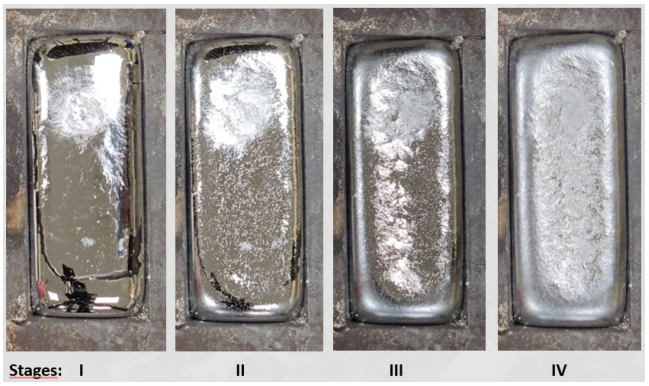

Fig. 9. Changes in the sample surface observed under visible light during the solidification of the alloy sample

Figures 10 and 11 show representative thermographic results of the top surface of the sample. These results (Figure 11) also confirm the effect of the change in shape and texture of the test surface on the thermogram as a result of the 4 previously described stages of changes in the emissivity of the sample surface.

A comparison of the thermographic curves of samples with different alloy densities shows that the results obtained are characteristic of the samples in terms of the shape and value of the temperature described. Analysis of the thermal emission data of the surface of the samples indicates that the values in the 4th stage of the solidification process of the samples are particularly repeatable.

The analysis was carried out for the designated rectangular 'Area 1' area of the sample surface thermogram. For each sample, the average temperature in the selected field during solidification was recorded and parameters such as the linear profile and histogram of the temperature distribution on the thermogram were analysed. In view of the above, a statistical analysis of the occurrence of a statistical relationship between the recorded average temperature and melt density was carried out.

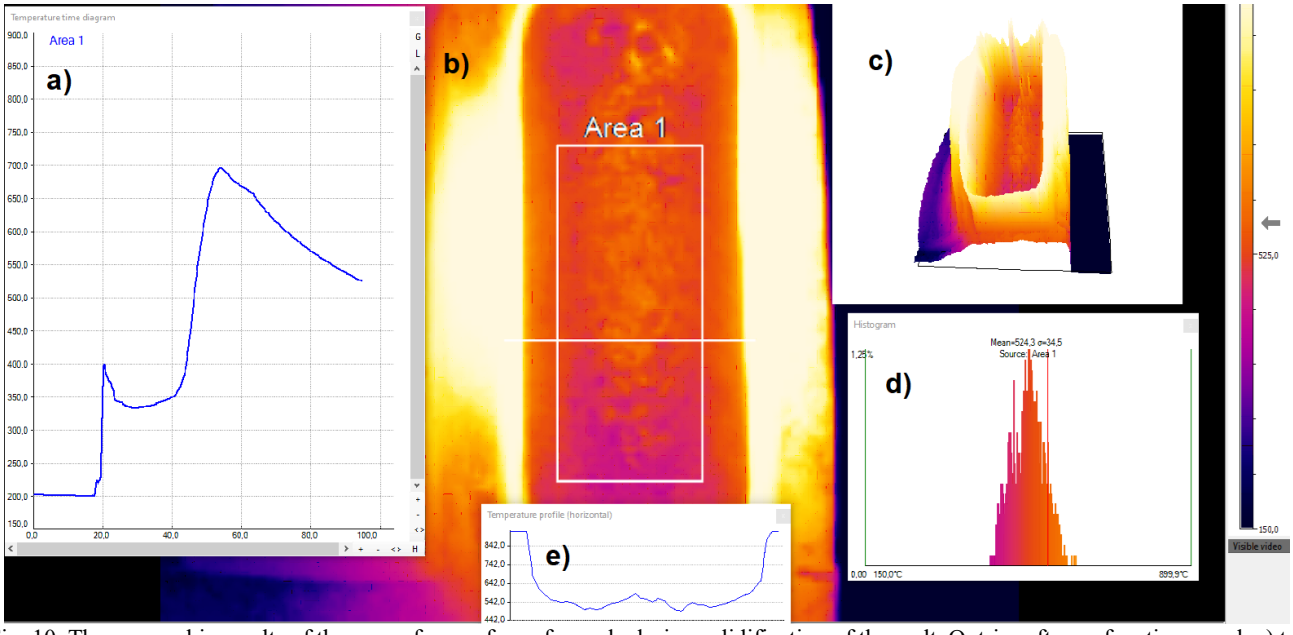

Fig. 10. Thermographic results of the upper free surface of sample during solidification of the melt. Optris software functions used: a) t = f(τ) of the thermal radiation average of "Area 1" area, b) - 2D thermogram of the analysed area, c) - 3D thermogram, d) - histogram of the temperature distribution in "Area 1", e) - temperature profile in the horizontal centre line of "Area 1" with radiometric values of: emissivity ε = 0,100 and transmissivity τ = 1,000

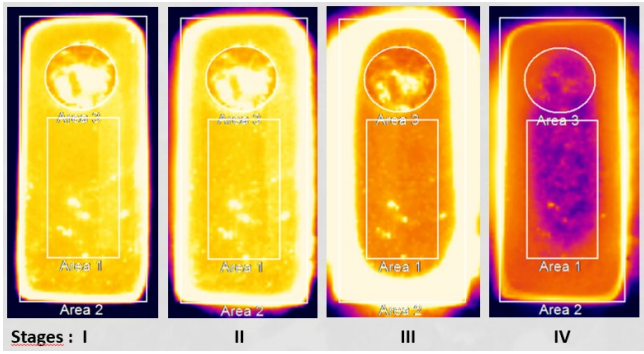

Fig. 11. Changes of thermal emission of the surface during the solidification of the alloy sample observed by infrared camera

Figure 12 shows the dot plot, the developed plotting model and its regression equation. The calculated value of the determination coefficient R^2 =0.92 confirms the high significance of the obtained model for the analyzed relationship.

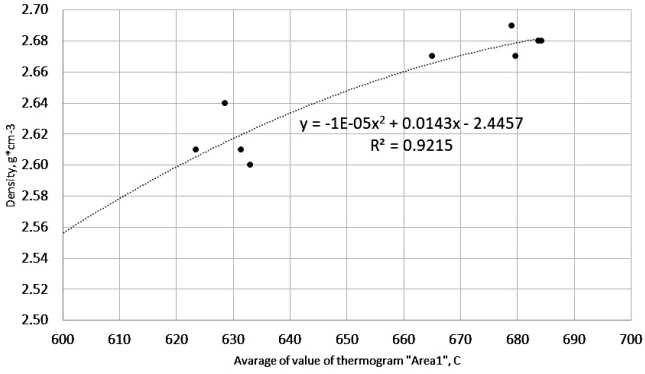

Fig. 12. Statistical relationship between average value of thermogram "Area 1" and alloy density

4. Conclusions

Analysis of the crystallisation process of the Al-Si alloy in the test die indicates that directionally solidifying samples enable studies of the density, based on thermographic analysis of the top surface of the sample. Quantitative differences in the porosity and impurities accumulated in the upper layer of the sample can be a factor determining the amount of heat flux recorded by the thermal imaging camera.

During the tests, changes in the shape and texture of the sample were observed, resulting from changes in the state of aggregation, solidification and casting shrinkage of the alloy. At the same time, these changes imply a variation in the thermal emissivity of the sample surface during thermographic analysis, which can make it difficult to accurately identify the sample temperature during solidification.

There is a statistical relationship between the characteristic value of the mean temperature of the surface thermogram field and the density of the alloy with a high coefficient of determination. This confirms the applicability of thermographic analysis to assess the quality of preparation of liquid Al-Si casting alloys.

The thermographic analysis of the free surface of the solidifying sample, provides a large amount of data that can be used as a basis for assessing the quality of liquid aluminium alloys in terms of the degree of density, gas dissolution degree of alloy and casting shrinkage.

References

[1] Dispinar, D., & Campbell, J. (2004). Critical assessment of reduced pressure test. Part 1: Porosity phenomena. *International Journal of Cast Metals Research*, 17(5), 280-286. https://doi.org/10.1179/136404604225020696.

[2] Kowalczyk W., Dańko R., Górny M., Kawalec M. & Burbelko A. (2022) Influence of High-Pressure Die Casting Parameters on the Cooling Rate and the Structure of EN-AC 46000 Alloy. *Materials*, 15(16), 5702. https://doi.org/10.3390/ma15165702.

[3] Y B Zuo, B Jiang, Y J Zhang & Z Fan. (2013). Degassing LM25 aluminium alloy by novel degassing technology with intensive melt shearing. *International Journal of Cast Metals Research*. 26(1), 16-21. doi: 10.1179/1743133612Y.0000000019.

[4] Pietrowski, S. (2001). *Al-Si Alloys.* Lodz, Poland: Wydawnictwo Politechniki Łódzkiej. ISBN 83-7283-029-0

[5] Gumienny, G., Pisarek, B., Szymczak, T., Gawroński, J., Just, P., Władysiak, R., Rapiejko, C. & Pacyniak, T. (2022). Effect of degassing parameters on mechanical properties of EN AC-46000 gravity die casting. *Materials*. 15(23), 8323, 1-13. https://doi.org/10.3390/ma15238323.

[6] Pietrowski, S., Gumienny, G., Pisarek, B. & Władysiak, R. (2004). Production control of advanced casting alloys with TDA method. *Archives of Mechanical Technology and Automation*. 24(3), 131-143, ISSN (1233-9709).

[7] Rapiejko C., Pisarek B., Czekaj E. & Pacyniak T., (2014). Analysis of AM60 and AZ91 Alloy Crystallization in Ceramic Moulds by Thermal Derivative Analysis (TDA). *Archives of Metallurgy and Materials*. 59, doi: 10.2478/amm-2014-0246.

[8] Gumienny G., Kurowska B. & Just P. (2019). The effect of Manganese on the Crystallization Process, Microstructure and Selected Properties of Compacted Graphite Iron. *Archives of Metallurgy and Materials*. 64(4), 1269-1275. doi: 10.24425/amm.2019.130090.

[9] Pisarek B., Rapiejko C. & Pacyniak T. (2019). Effect of intensive Cooling of Alloy AC-AlSi7Mg with Alloy additions on Microstructure and Mechanical Properties. *Archives of Metallurgy and Materials.* 64 (2), 677-681. DOI: 10.2478/amm-2019.127598.

[10] Władysiak, R. & Kozuń, A. (2015). An Application for Infrared Camera in Analyzing of the Solidification Process of Al-Si Alloys. *Archives of Foundry Engineering*. 15(3), 81-84. DOI: 10.1515/afe-2015-0065.

[11] Holtzer, M., Bobrowski, A., Grabowska, B., Eichholz, S. & Hodor, K. (2010). Investigation of carriers of lustrous carbon at high temperatures by infrared spectroscopy (FTIR). *Archives of Foundry Engineering*. 10(4), 61-68.

[12] Sapieta, M., Dekys, V., Kao, M., Pastor, M., Sapietova, A. & Drvarova, B. (2023). Investigation of the mechanical properties of spur involute gearing by infrared thermography. *Applied Sciences*. 13(10), 5988. https://doi.org/10.3390/app13105988.

[13] Umar M. &·Paulraj S. (2021). Thermography analysis and porosity formation during laser beam welding of AA5083-H111 aluminum alloy. *Journal of Thermal Analysis and Calorimetry* 146, 1551–1559. https://doi.org/10.1007/s10973-020-10140-z.

[14] Lanc Z., Strbac B., Zeljkovic M., Zivkovic A. & Hadzistevic M. (2018). Emissivity of Aluminium Alloy Using Infrared Thermography Technique. *Materials and Technology.* 52(3). doi:10.17222/mit.2017.152.

[15] Badulescu C., Grediac M., Haddadi H., Mathias J.-D., Balandraud X. & Tran H.-S. (2011) Applying the Grid Method and Infrared Thermography to Investigate Plastic deformation in Aluminium Multicrystal. *Mechanics of Materials*, 43(1), 36-53. doi:10.1016/j.mechmat.2010.11.001.